Binding and mucoadhesion of sulfurated derivatives of quaternary ammonium-chitosans and their nanoaggregates: an NMR investigation

Andrea Cesari[a], *Angela Fabiano*[b], *Anna Maria Piras*[b], *Ylenia Zambito*[b], *Gloria Uccello-Barretta*[a], *Federica Balzano*[a]*

[a]*Department of Chemistry and Industrial Chemistry, University of Pisa, via Moruzzi 13, 56124 Pisa, Italy*

[b]*Department of Pharmacy, University of Pisa, via Bonanno 33, 56126 Pisa, Italy*

Abstract

The effect of insertion of SH and *S*-protected groups on the binding and mucoadhesion properties of quaternary ammonium-chitosans and their nanoparticulate forms has been investigated by NMR spectroscopy. Diclofenac sodium salt has been assumed as low molecular weight probe to detect the different binding behaviour of polymeric materials; mucin from bovine submaxillary glands was selected as the model protein for differentiating their mucoadhesion. NMR proton selective relaxation rates of the probe molecule were remarkably sensitive to the presence of very low amounts of sulfurated moieties. Impact of supramolecular aggregation in nanostructured species was demonstrated as well as the relevance of *S*-protection.

Keywords

Thiolated chitosan, Nanoparticles, Mucoadhesion, Nuclear magnetic resonance, Selective relaxation rate

1. Introduction

Among natural polysaccharides, chitosan (Fig. 1) represents a promising semi-synthetic polymer used in diverse fields, spanning from agricultural to biomedical uses. In virtue of its low cost, low toxicity and desirable pharmaceutical properties, such as antimicrobial activity [1] and biocompatibility [2], it has been the subject of ever-increasing interest in the biopharmaceutical industry. Chitosan itself can be used as dietary supplement and in wounds healing, or in combination with specific drugs, exploiting its polymeric scaffold as a carrier [3]. It is easily accessible upon chemical deacetylation (enzymatic deacetylations have also been reported [4]) of the abundant polysaccharide chitin, giving chitosans of different degrees of deacetylation. In addition to varying the molecular weight and degree of deacetylation, several chemical

modifications have been proposed to affect chitosan physicochemical properties. The reactive NH and OH free groups, present in the sugar ring units, are readily accessible to formation of covalent bonds, hence, different modified chitosans have been proposed, such as *O*- and *N*-carboxymethyl, *N*-methylene phosphonic or cyclodextrin-grafted chitosans [5,6]. Taking into account the potentialities of nanoparticles formulations, chitosans can also be assembled into nanodimensional aggregates using different preparation protocols, including ionotropic gelation carried out with hyaluronic acid [7]. The functional groups on the polymer backbone influence the surface characteristics of the relative nanoparticles, which in turn influence their ability to interact with biological systems, for example promoting their mucoadhesive properties and their tendency to be internalized by cells. In this regard, the synthesis of an ammonium alkylated chitosan (Fig. 1) upon reaction with 2-diethylaminoethyl chloride (DEAE-Cl) has been proposed [8]. The resulting derivative showed improved antibacterial and drug permeation promoting properties, with respect to the chitosan precursor.

Thiolated polymers or thiomers (Fig. 1) can exert a sustained mucoadhesion by covalent interaction through disulfide bonds with the cysteine rich domains of mucin [9]. However, SH groups in the polymer backbone undergo oxidation and their reactivity is strongly pH dependent. This has led to a second generation of thiomers, with *S*-protected moieties [9,10], where also 6-mercaptonicotinamide was exploited to preserve SH groups from oxidative processes and to pre-activate the polymer towards mucin (Fig.1).

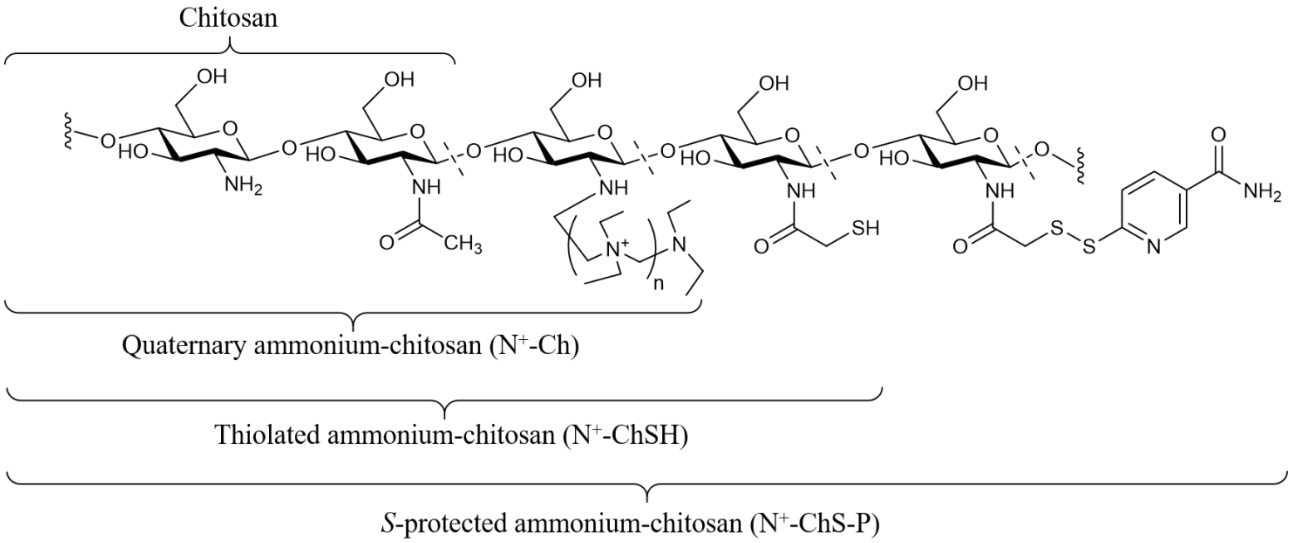

Fig. 1. Schematic representation of the different units in chitosan and in its derivatives.

Several methods have been developed to study mucoadhesion *in vitro*, which can be divided into methods based on either mechanical forces determination or particles interaction analysis [11]. Among the latter, ellipsometry and rheology are two relatively simple techniques, but strongly dependent on experimental conditions [12]. Nuclear magnetic resonance spectroscopy (NMR) represents a powerful non-invasive technique with promising perspectives in the field of the investigation of affinity properties of macromolecules [13]. In particular, proton selective relaxation rates, as remarkably responsive NMR

parameters [14], have been successfully applied to the study of mucoadhesion of polysaccharide materials [15–18].

Here we report on the results of our NMR investigation on affinity and mucoadhesion properties of chitosan derivatives and their nanoparticulate aggregates, by comparing quaternary ammonium-chitosan conjugates and their thiolated and *S*-protected derivatives (Fig. 1). Chitosan of reduced molecular weight was chosen as the substrate for further derivatization and nanoparticles preparation [19]. Diclofenac sodium salt (DC) was selected as a low molecular weight sensitive probe, the relaxation properties of which were affected by the interaction with the polysaccharide and/or mucin, as detected by comparing its proton selective relaxation rates in binary mixtures, drug/polymer, and ternary systems, drug/polymer/mucin. The effect of polymers assembly into nanoparticulate structures on mucoadhesion has also been taken into consideration. Diffusion coefficients measured by the NMR DOSY (Diffusion Ordered SpectroscopY) technique [20,21] have been employed as additional NMR parameters, responsive to the slowing down of the translational molecular motion of the probe compound (DC) due to the interaction with the polymeric materials and their nanoaggregates.

2. Materials and Methods

2.1. Materials

Chitosan from shrimp shells (75-85% deacetylated), diclofenac sodium salt (DC), thiourea, 6-chloronicotinamide, reduced glutathione, *N*-(3-dimethylaminopropyl)-*N*'-ethylcarbodiimide chloridrate (EDAC), 5,5'-dithiobis-(2-nitrobenzoic) acid (Ellman's reagent), thioglycolic acid, mucin from bovine submaxillary glands (BSM), 2-diethylaminoethyl chloride hydrochloride salt (DEAE-Cl·HCl), tetramethylsilane (TMS), phosphate buffer powder (PB, pH = 7.4) were purchased from Sigma Aldrich (St. Louis, Missouri, US). Deuterated water (D_2O) was purchased from Deutero GmbH (Kastellaun, Germany). Hyaluronic acid (HA) was purchased from Contipro (Dolní Dobrouc, Czech Republic).

2.2 Instruments

The molecular weights of reduced chitosan and reduced hyaluronic acid were determined by an Ostwald U-tube capillary viscometer Cannon-Fenske series ASTM 75 (State College, PA, US).

The lyophilization of both polymers and nanoparticles was conducted by VirTis Advantage (SP industries, Warminster, PA, US). The temperature cycle was set at -35 °C/180 min, -30 °C/360 min under vacuum, -10 °C/360 min, 10 °C/240 min and 25 °C/180 min.

Light Scattering measurements were recorded using N4 plus DLS (Beckman Coulter, Brea, CA, US) selecting angles of 90° and 62.6°.

NMR measurements were performed on Varian INOVA 600 spectrometer operating at 600 MHz for ^{1}H. The temperature was controlled to 25±0.1 °C. Proton 2D gCOSY (gradient COrrelated SpectroscopY) spectra were recorded with 256 increments of 4 scans and 2k data points. The relaxation delay was 1 s. The 2D NOESY (Nuclear Overhauser Effect SpectroscopY) spectra were acquired with 2k data points using 8 scans for each of the 256 t_1 increments, with a mixing time of 0.6 s and a relaxation delay of 1 s. The spin-lattice selective

relaxation times were measured in the initial rate approximation [22] by using the inversion recovery pulse sequence $(180°\text{-}\tau\text{-}90°\text{-}t)_n$ with a selective π-pulse at the selected frequency and a relaxation delay of 15 s. DOSY (Diffusion Ordered SpectroscopY) experiments were carried out by using a stimulated echo sequence with self-compensating gradient schemes and 64k data points. Typically, gradient strength was varied in 20 steps (2–32 transients each), delays Δ and δ were optimized in order to obtain an approximately 90–95% decrease in the resonance intensity at the largest gradient amplitude. The baselines of all arrayed spectra were corrected prior to processing the data. After data acquisition, each FID was apodized with 1.0 Hz line broadening and Fourier transformed. Gradient amplitudes in DOSY experiments have been calibrated by using a standard sample of D_2O 99% (19×10^{-10} m^2s^{-1}). TMS was used as viscosity reference.

2.3 Modified chitosans preparation

Reduced molecular weight chitosan (Ch) was obtained by $NaNO_2$ oxidative degradation in acidic media of commercial chitosan (400 kDa, viscosimetric determination) as described by Shu et al. [23]. The mean molecular weight of Ch was determined by using a capillary viscometer (136 kDa), as reported by Khalid et al. [24]. Quaternarized Ch (N^+-Ch, [8]), thiolated Ch (N^+-ChSH, [19]) and *S*-protected Ch (N^+-ChS-P, [10]), were prepared by previously reported procedures.

Degree of acetylation (11.7%), degree of derivatization (47.1%) and charged to neutral nitrogen ratio (2.1) of amino alkyl derivatizing group of the N^+-Ch precursor were calculated by a previously developed NMR analytical protocol [25].

The amount of sulfurated moieties in N^+-ChSH and N^+-ChS-P were determined by iodimetric titration [10] and Ellman test [26], respectively. The total free sulfhydryl moieties were quantified in N^+-ChSH with a $NaBH_4$ pre-reduction, giving 175 μmol/g (2.4%), while in the non-pretreated N^+-ChSH sample the free thiols amount was 66.2 μmol/g (0.9%). The content of free thiols in non-pretreated N^+-ChS-P was lowered down to 9 μmol/g (0.3%) by the introduced aromatic groups. Specifically, N^+-ChS-P was furtherly analysed determining the effective amount of protective group grafted [10]: solution of reduced glutathione was added to N^+-ChS-P solution to release the 6-mercaptonicotinamide (6-MNA). Measuring the absorbance of the released aromatic ligand and referring to the calibration curve for 6-MNA (r^2=0.9992, n=5), the ligand was quantified as 53 μmol per gram of N^+-ChS-P, in good agreement with that determined by comparing free thiols quantification in N^+-ChSH (66.2 μmol/g) and in N^+-ChS-P (9 μmol/g).

2.4 Nanoparticles preparation

Depolymerized hyaluronic acid (rHA), which was employed as reticulating agent, was obtained according to the procedure described by Shu et al. [23] starting from commercial hyaluronic acid (M_w=950 kDa) in acidic condition (M_w=87 kDa, by viscosimetric determination). Nanoparticles were prepared by dropwise adding a solution of rHA (phosphate buffer 0.13 M, pH=7.4, 0.06 mg/mL for N^+-Ch, and 0.03 mg/mL for N^+-ChSH and N^+-ChS-P) to the corresponding 2 mg/mL polymer solution in the same buffer, under magnetic stirring. The nanoparticles could be regenerated from the respective lyophilized products by adding 5 mL of water under gentle stirring. Nanoparticles sizes as determined by Dynamic Light Scattering were less than 500 nm for all

of the three polymers [Np^{N+-Ch} 434.0 nm - (0.493), $Np^{N+-ChSH}$ 479.0 nm - (0.376), $Np^{N+-ChS-P}$ 403.9 nm - (0.363)], where polydispersity indexes are reported in round parenthesis.

2.5 NMR samples preparation

Binary and ternary mixtures employed for NMR studies were prepared by mixing appropriate amounts of stock solutions (D_2O/PB) of each component for analysis concentration of 0.4 mg/mL for DC, 1.2 mg/mL for polymer or nanoparticles and/or 3 mg/mL for mucin. Mixtures were analysed after 2 hours of vortexing (500 rpm) at 37 °C and an hour of equilibration at room temperature.

3. Results and Discussion

For the complexation equilibrium (1) between a ligand (L) and a macromolecule (M), a single set of NMR signals for the ligand is detected in the fast exchange condition and the observable NMR parameters (P_{obs}) are the weighted average between the bound (P_b) and free (P_f) states (Eq. (2)).

$$L + M \rightleftarrows LM \quad (1)$$

$$P_{obs} = \chi_f P_f + \chi_b P_b \quad (2)$$

where χ_f and χ_b are the molar fractions of the ligand in the free and bound states, respectively.
As the consequence of the remarkable difference between the molecular weight of the ligand and the macromolecule, very high ligand-to-receptor molar ratios are commonly employed, in order to obtain observable signals of the ligand. Therefore, changes in the parameters are only detected when their values in the bound state are remarkably differentiated from those in the free state.
Among NMR parameters, proton mono-selective spin-lattice relaxation rates ($R_i^{ms} = 1/T_i^{ms}$), which are measured by following the recovery of the magnetization of the spin i selectively inverted, are strongly responsive to the slowing down of the molecular motion of the ligand due to its complexation at receptor site. In particular, these parameters undergo a sharp increase in the slow motion region ($\omega^2\tau_c^2 \gg 0.6$, where ω is the Larmor frequency and τ_c the rotational correlation time), which is typical of small molecules bound to macromolecules. By contrast, the corresponding non-selective relaxation rates ($R_i^{ns} = 1/T_i^{ns}$), which are measured by following the recovery of i magnetization under simultaneous inversion of the complete spins system, are scarcely sensitive to the change of motion regime due to the complexation.
In addition, the cross-relaxation term, σ_{ij}, referred to the dipolar interaction between the magnetic moments of the two spins, i and j at r_{ij} distance, represents a very useful NMR parameter in the detection of the interaction between a small molecule and a macromolecule. In particular, in the two limit regions of fast motion ($\omega^2\tau_c^2 \ll 0.6$) and slow motion ($\omega^2\tau_c^2 \gg 0.6$), corresponding to the free and bound states of the ligand, σ_{ij} can be approximated to the simple forms reported in Equations (3) and (4), respectively.

$$\sigma_{ij} = 0.5\ \gamma^4\ \hbar^2\ r_{ij}^{-6}\ \tau_c \quad (\omega^2\tau_c^2 \ll 0.6) \quad (3)$$

$$\sigma_{ij} = -0.1\ \gamma^4\ \hbar^2\ r_{ij}^{-6}\ \tau_c \quad (\omega^2\tau_c^2 \gg 0.6) \tag{4}$$

The cross-relaxation term varies from positive values, in the fast motion regime of the free ligand, to negative ones, characteristic of slow motion regime of the ligand induced by macromolecule binding. σ_{ij} can be straightforwardly calculated as the difference between the bi-selective relaxation rate and the mono-selective relaxation rate of the spin *i* (Eq. (5)), where bi-selective relaxation rates ($R^{bs}_{i,j} = 1/T^{bs}_{i,j}$) are determined by following the recovery of the magnetization of the spin *i* under simultaneous inversion of the proton pair H_i/H_j.

$$\sigma_{ij} = R^{bs}_{i,j} - R_i^{ms} \tag{5}$$

The diffusion coefficient *D* (m^2s^{-1}), which describes the molecular translational motion, represents another parameter that can be usefully exploited to detect the interaction between a small molecule and a macromolecule. The dependence of this parameter from the hydrodynamic radius (r_H) and viscosity (η) can be expressed by means of the Stokes–Einstein equation (Eq. (6)), strictly holding for spherical molecules

$$D = k_bT / (6\ \pi\ \eta\ r_H) \tag{6}$$

where k_b is the Boltzmann constant, and *T* is the absolute temperature. When a molecule interacts with a macromolecule, an increase of its hydrodynamic radius is expected and, hence, a decrease of the diffusion coefficient, which can be detected by using the NMR DOSY technique. In order to exclude effects arising from viscosity increment of the medium upon addition of high molecular weight polymer, an internal viscosity standard must be selected [27].

Diclofenac sodium salt (DC) has a simple chemical structure, very good water solubility and its aromatic resonances (Fig. 2) are well separated in a spectral region with no interferences by signals arising from the polymeric materials. DC resonances of ring A have been simply assigned on the basis of the integrated areas and multiplicity. Regarding ring B, proton H_6 has been assigned due its dipolar interaction with methylene chain protons detected in the NOESY map (Fig. S1, Supplementary material). Scalar correlations detected in the COSY map (Fig. S2, Supplementary material) starting from H_6 allowed us to assign all the spins system of ring B, as indicated in Figure 2.

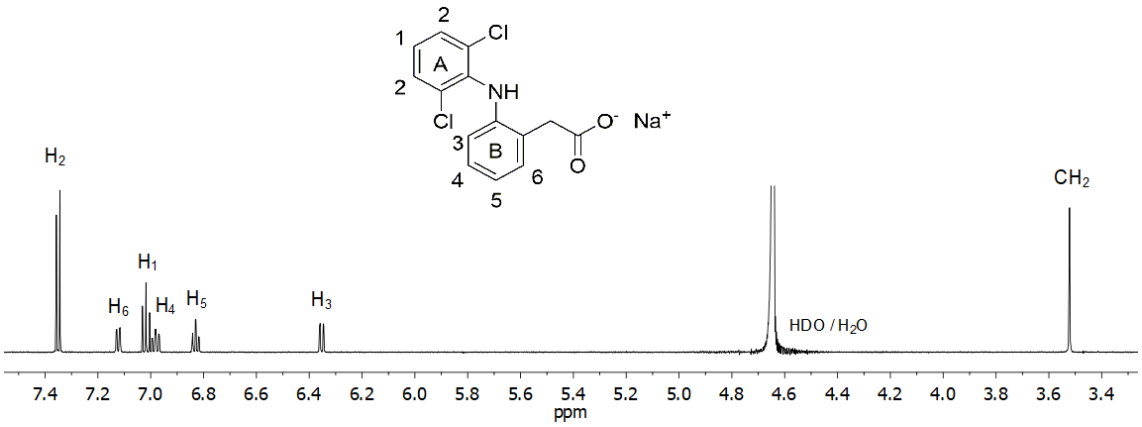

Fig. 2. ^{1}H NMR (600 MHz, D_2O/PB, pH = 7.4, 25 °C) spectrum of DC (0.4 mg/mL).

Firstly, we measured proton selective relaxation rates in D_2O solution of DC (0.4 mg/mL), focusing on proton H_2 on A ring and protons H_6, H_5 and H_3, belonging to B ring (Table 1). All of these protons produce well separated resonances in the ^1H NMR spectrum and, hence, can be selectively inverted. The corresponding non-selective relaxation parameters R_i^{ns} are collected in Table S1 (Supplementary material). By measuring the bi-selective relaxation rate of proton H_3 under simultaneous inversion of proton H_4, the cross-relaxation term σ_{34} of 0.05 s^{-1} was calculated. Both relaxation values and cross relaxation term are as expected for a small molecule in the fast motion region. As a matter of fact, on the basis of approximate Equation 3, the rotational correlation time of 0.04 ns was calculated for the vector connecting protons H_3 and H_4 (assuming r_{34} = 2.49 Å as the typical distance of two vicinal aromatic protons [28]). The presence of phosphate buffer (0.1 M) did not produce changes of NMR relaxation parameters of DC with respect to the D_2O solution.

The solutions containing DC and the modified chitosans (for ^1H NMR spectra of the modified polymers see Figure S3, Supplementary material), were analysed after vortexing of the mixtures for 2 hours at 37 °C and stabilization of the solutions at 25 °C for 1 hour. Due to the presence of the ammonium-chitosan of reduced molecular weight (N^+-Ch), a marked increase of proton selective relaxation rates was detected: as an example, the relaxation rate of proton H_3, which was 0.23 s^{-1} in pure DC, increased to 2.22 s^{-1} in the mixture containing 1.2 mg/mL of polymer. Similar increases of the selective relaxation rates of protons H_6, H_5 and H_2 were detected (Table 1). Interestingly, the cross-relaxation term σ_{34} underwent a sign change to the value of -0.77 s^{-1}, which was indicative of a clear slowing down of the molecular motion of DC due to its interaction with the polymer, accordingly approximate Equation 4 gave the corresponding τ_c value of 3.22 ns. DC diffusion coefficient underwent a significant decrease in the presence of the polymer from 5.4 x 10^{-10} m^2s^{-1} in pure DC to 4.4 x 10^{-10} m^2s^{-1} in the binary mixture DC/ N^+-Ch. Possible effects of viscosity changes both on relaxation rates and diffusion coefficients were ruled out by selecting tetramethylsilane as the internal standard, the diffusion coefficient and relaxation rate of which remained relatively unchanged in the solutions containing pure DC and its mixture with the polymer (Table S2, Supplementary material). On the contrary, proton non-selective relaxation rates were scarcely responsive to the presence of the polymer (Table S1, Supplementary material).

Table 1. Mono-selective relaxation rates (R_1^{ms}, s^{-1}) of H_2, H_3, H_5 and H_6 protons of DC (600 MHz, D_2O/PB, pH = 7.4, 25 °C, 0.4 mg/mL) and cross-relaxation parameter (σ_{34}, s^{-1}) in different mixtures, after 2 hours of continuous stirring at 37 °C and 1 hour of equilibration at room temperature.

	δ (ppm)	R_1^{ms} (s^{-1})			
		DC	DC/N^+-Ch	DC/N^+-ChSH	DC/N^+-ChS-P
H_2	7.35	0.18	1.57	1.06	1.07
H_3	6.34	0.23	2.22	1.62	1.51
H_5	6.84	0.32	2.70	1.95	1.85
H_6	7.12	0.36	2.74	2.02	1.99
		σ_{34} (s^{-1})			
H_3/H_4		0.05	-0.77	-0.55	-0.52

Measurements were repeated after 24 hours at room temperature and no significant changes of relaxation rates were detected, to indicate that NMR parameters were not affected by conformational stabilization of the polymeric materials over time (Table S3, Supplementary material).

In this regard it is noteworthy that very different results were obtained in the mixtures containing non-reduced molecular weight ammonium-chitosan: lower relaxation rates with respect to reduced molecular weight system were measured after 2 hours of vortexing and 1 hour of stabilization, but these values remarkably increased after 24 hours, as the consequence of slow conformational stabilization phenomena occurring over time (Table S3, Supplementary material).

In the above said standardized conditions for reduced molecular weight polymers, selective relaxation rates of DC protons in binary mixtures containing thiolated ammonium-chitosan (N^+-ChSH) and its *S*-protected derivative (N^+-ChS-P) were analysed (Table 1). Despite the very low content of SH (0.9 %) or *S*-protected groups (0.6%), a significant change of selective relaxation rates was detected with respect to the parent ammonium-chitosan derivative. As an example, relaxation parameter of proton H_3 decreased from 2.22 s^{-1} for DC/N^+-Ch to 1.62 s^{-1} for DC/N^+-ChSH and 1.51 s^{-1} for DC/N^+-ChS-P. A significant effect was also detected in the cross-relaxation term σ_{34}, which changed from -0.77 s^{-1} (DC/N^+-Ch) to -0.55 s^{-1} (DC/N^+-ChSH) or to -0.52 (DC/N^+-ChS-P). These data reflect the diminished capability of thiolated polymers to bind DC, which must reasonably be ascribed to conformational changes triggered by the modification of thiol groups rather than by their mere presence.

Supramolecular assembly of polymers in the form of nanoparticles ($Np^{N+\text{-}Ch}$, $Np^{N+\text{-}ChSH}$ and $Np^{N+\text{-}ChS\text{-}P}$) remarkably affected binding ability of the three polymers, since relaxation rates of DC protons underwent remarkable increases in the binary mixtures containing empty nanoparticles with respect to the polymers (Tables 1, 2). To make a reliable comparison, the polymer concentration in the nanoparticles sample was kept constant to the binary mixture containing the same polymer. A reproducible decreasing trend was observed for proton selective relaxation rates from $Np^{N+\text{-}Ch}$ to $Np^{N+\text{-}ChS\text{-}P}$ (Table 2). Interestingly,

supramolecular assembly into nanoparticulate form allowed us to differentiate the thiolated system (5.10 s^{-1} for H_3) from the *S*-protected one (2.57 s^{-1} for H_3). On considering that interaction with empty nanoparticles occurs at their external surface, a lower binding ability of empty $Np^{N+\text{-}ChS\text{-}P}$ means an enhanced availability of the drug after the release for targeted interactions with biological matrices.

Table 2. Mono-selective relaxation rates (R_1^{ms}, s^{-1}) of H_2, H_3, H_5 and H_6 protons of DC (600 MHz, D_2O/PB, pH = 7.4, 25 °C, 0.4 mg/mL) and cross-relaxation parameter (σ_{34}, s^{-1}) in different DC/nanoparticles mixtures, after 2 hours of continuous stirring at 37 °C and 1 hour of equilibration at room temperature.

	δ (ppm)	R_1^{ms} (s^{-1})			
		DC	DC/$Np^{N+\text{-}Ch}$	DC/$Np^{N+\text{-}ChSH}$	DC/$Np^{N+\text{-}ChS\text{-}P}$
H_2	7.35	0.18	4.20	3.25	1.57
H_3	6.34	0.23	6.68	5.10	2.57
H_5	6.84	0.32	6.78	5.67	3.07
H_6	7.12	0.36	7.78	5.78	3.18
		σ_{34} (s^{-1})			
H_3/H_4		0.05	-3.57	-2.34	-0.99

As a model of the interactions responsible for mucoadhesion, bovine submaxillary mucin (BSM) was chosen and its interaction with DC in the presence or absence of polymeric material was compared. Binding ability of mucin towards DC was remarkably higher as revealed by the values of proton selective relaxation rates (8.28 s^{-1} and 8.56 s^{-1} for H_2 and H_3 respectively in the mixture containing 3 mg/mL of BSM, Table 3). In these mixtures only H_2 and H_3 relaxation parameters were evaluated, the resonances of which did not suffer from superimposition due to mucin signals. The copresence of chitosans and mucin in the ternary mixtures strongly affected proton selective relaxation rates of DC (Table 3), with changes always higher than the simple sum of the values measured in the corresponding binary mixtures (Tables 1-3). This indicates a synergistic interaction between modified chitosans and mucin. As an example, the value of 14.25 s^{-1} was measured for the proton H_2 in the ternary mixture DC/N^+-Ch/BSM (Table 3) to be compared to 9.85 s^{-1}, corresponding to the sum of the values measured for the binary systems DC/BSM (8.28 s^{-1}, Table 3) and DC/N^+-Ch (1.57 s^{-1}, Table 1). The relaxation rates measured in the ternary mixture DC/N^+-ChSH/BSM and DC/N^+-ChS-P/BSM were both lower (11.21 s^{-1} and 13.28 s^{-1}, respectively) than the value obtained for the ternary mixture containing the parent ammonium-chitosan (Table 3). However, the real cooperation between the two polymeric materials has to be evaluated from the difference between relaxation rate in ternary system and in the binary one, normalized by the binary mixture ($\Delta_{BSM} = [R_1^{ms}(T) - R_1^{ms}(B)]/R_1^{ms}(B)$), which are reported in Table 3). The above said values are remarkably higher for the sulfurated chitosans than for the

ammonium-chitosan. Between the two sulfurated systems, the protected polymer showed the major cooperation (Table 3).

Table 3. Mono-selective relaxation rates (R_1^{ms}, s^{-1}) of H_2 and H_3 proton of DC (600 MHz, D_2O, pH = 7.4, 0.4 mg/mL), relaxation rates increment (Δ_{BSM}) in different BSM mixtures, after 2 hours of continuous stirring at 37 °C and equilibration at room temperature.

Sample	H_2		H_3	
	R_1^{ms}	Δ_{BSM}	R_1^{ms}	Δ_{BSM}
DC/BSM	8.28	-	8.56	-
DC/N^+-Ch/BSM	14.25	8.08	16.15	6.27
DC/N^+-ChSH/BSM	11.21	9.57	11.58	6.16
DC/N^+-ChS-P/BSM	13.28	11.41	15.50	9.26
DC/Np^{N+-Ch}/BSM	10.44	1.49	12.77	0.92
DC/$Np^{N+-ChSH}$/BSM	13.63	3.19	13.70	1.69
DC/ $Np^{N+-ChS-P}$/BSM	9.34	4.95	12.70	3.94

The same trend was found in the case of ternary mixtures containing the nanoparticles, where Δ_{BSM} was higher for the *S*-protected system $Np^{N+-ChS-P}$, and lower for the nanoparticles Np^{N+-Ch} formed from the parent quaternary ammonium-chitosan (Table 3). Therefore, protection of SH moieties is beneficial also for the nanostructured systems with respect to its unprotected precursor. It is noteworthy that nanoparticles perturbed the interaction of DC with mucin to a lesser extent than the corresponding polymers. This could be attributed to the available contact surface being smaller with the nanoparticulate systems than with their parent polymers.

4. Conclusions

Proton selective relaxation rate measurements constitute a powerful non-invasive investigation tool to detect drug to polymer binding, in virtue of their remarkable responsivity to the changes of motion regime of small molecules as the consequence of their interaction with macromolecular systems. By exploiting this important property, significant differences were detected in the binding ability of diclofenac to quaternary ammonium-chitosans containing free SH groups or *S*-protected ones, in spite of the very low amounts of sulfurated moieties. NMR parameters allowed us to differentiate the binding and mucoadhesion properties of nanoparticulated forms of chitosans with respect to the corresponding polymers, highlighting the relevance of *S*-protection on the mucoadhesion of sulfurated chitosans.

Acknowledgments

The work was supported by University of Pisa (PRA_2018_23 “Functional Materials”).

References

[1] M. Kong, X.G. Chen, K. Xing, H.J. Park, Antimicrobial properties of chitosan and mode of action: A state of the art review, International Journal of Food Microbiology. 144 (2010) 51–63. doi:10.1016/j.ijfoodmicro.2010.09.012.

[2] M. Dash, F. Chiellini, R.M. Ottenbrite, E. Chiellini, Chitosan - A versatile semi-synthetic polymer in biomedical applications, Progress in Polymer Science (Oxford). 36 (2011) 981–1014. doi:10.1016/j.progpolymsci.2011.02.001.

[3] J.H. Park, G. Saravanakumar, K. Kim, I.C. Kwon, Targeted delivery of low molecular drugs using chitosan and its derivatives, Advanced Drug Delivery Reviews. 62 (2010) 28–41. doi:10.1016/j.addr.2009.10.003.

[4] I. Tsigos, A. Martinou, D. Kafetzopoulos, V. Bouriotis, Chitin deacetylases: new, versatile tools in biotechnology, Trends in Biotechnology. 18 (2000) 305–312. doi:10.1016/S0167-7799(00)01462-1.

[5] A.M. Piras, Y. Zambito, S. Burgalassi, D. Monti, S. Tampucci, E. Terreni, A. Fabiano, F. Balzano, G. Uccello-Barretta, P. Chetoni, A water-soluble, mucoadhesive quaternary ammonium chitosan-methyl-β-cyclodextrin conjugate forming inclusion complexes with dexamethasone, Journal of Materials Science: Materials in Medicine. 29 (2018). doi:10.1007/s10856-018-6048-2.

[6] V.K. Mourya, N.N. Inamdar, Chitosan-modifications and applications: Opportunities galore, Reactive and Functional Polymers. 68 (2008) 1013–1051. doi:10.1016/j.reactfunctpolym.2008.03.002.

[7] A.M. Piras, G. Maisetta, S. Sandreschi, S. Esin, M. Gazzarri, G. Batoni, F. Chiellini, Preparation, physical-chemical and biological characterization of chitosan nanoparticles loaded with lysozyme, International Journal of Biological Macromolecules. 67 (2014) 124–131. doi:10.1016/j.ijbiomac.2014.03.016.

[8] Y. Zambito, C. Zaino, G. Uccello-Barretta, F. Balzano, G. Di Colo, Improved synthesis of quaternary ammonium-chitosan conjugates (N+-Ch) for enhanced intestinal drug permeation, European Journal of Pharmaceutical Sciences. 33 (2008) 343–350. doi:10.1016/j.ejps.2008.01.004.

[9] S. Dünnhaupt, J. Barthelmes, C.C. Thurner, C. Waldner, D. Sakloetsakun, A. Bernkop-Schnürch, S-protected thiolated chitosan: Synthesis and in vitro characterization, Carbohydrate Polymers. 90 (2012) 765–772. doi:10.1016/j.carbpol.2012.05.028.

[10] A. Fabiano, A.M. Piras, G. Uccello-Barretta, F. Balzano, A. Cesari, L. Testai, V. Citi, Y. Zambito, Impact of mucoadhesive polymeric nanoparticulate systems on oral bioavailability of a macromolecular model drug, European Journal of Pharmaceutics and Biopharmaceutics. 130 (2018) 281–289. doi:10.1016/j.ejpb.2018.07.010.

[11] M. Davidovich-Pinhas, H. Bianco-Peled, Mucoadhesion: a review of characterization techniques, Expert Opinion on Drug Delivery. 7 (2010) 259–271. doi:10.1517/17425240903473134.

[12] H. Hägerström, K. Edsman, Limitations of the rheological mucoadhesion method: The effect of the choice of conditions and the rheological synergism parameter, European Journal of Pharmaceutical Sciences. 18 (2003) 349–357. doi:10.1016/S0928-0987(03)00037-X.

[13] L. Fielding, NMR Methods for the Determination of Protein- Ligand Dissociation Constants, Current Topics in Medicinal Chemistry. 3 (2003) 39–53. doi:10.2174/1568026033392705.

[14] G. Valensin, G. Sabatini, E. Tiezzi, Determination of Zero- and Double-Quantum Relaxation Transition Probabilities by Multiple-Selective Irradiation Methods, in: N. Niccolai, G. Valensin (Eds.), Advanced Magnetic Resonance Techniques in Systems of High Molecular Complexity, Birkhäuser Boston, Boston, MA, 1986: pp. 69–76. doi:10.1007/978-1-4615-8521-3_6.

[15] G. Uccello-Barretta, F. Balzano, F. Aiello, A. Senatore, A. Fabiano, Y. Zambito, Mucoadhesivity and release properties of quaternary ammonium–chitosan conjugates and their nanoparticulate supramolecular aggregates: An NMR investigation, International Journal of Pharmaceutics. 461 (2014) 489–494. doi:10.1016/j.ijpharm.2013.12.018.

[16] F. Aiello, F. Balzano, L. Carpita, A. Fabiano, Y. Zambito, G. Uccello Barretta, Role of nanostructured aggregation of chitosan derivatives on [5-methionine]enkephalin affinity, Carbohydrate Polymers. 157 (2017) 321–324. doi:10.1016/j.carbpol.2016.09.089.
[17] G. Uccello-Barretta, F. Balzano, L. Vanni, M. Sansò, Mucoadhesive properties of tamarind-seed polysaccharide/hyaluronic acid mixtures: A nuclear magnetic resonance spectroscopy investigation, Carbohydrate Polymers. 91 (2013) 568–572. doi:10.1016/j.carbpol.2012.07.085.
[18] G. Uccello-Barretta, S. Nazzi, F. Balzano, M. Sansò, A nuclear magnetic resonance approach to the comparison of mucoadhesive properties of polysaccharides for ophthalmic uses, International Journal of Pharmaceutics. 406 (2011) 78–83. doi:10.1016/j.ijpharm.2010.12.032.
[19] Y. Zambito, F. Felice, A. Fabiano, R. Di Stefano, G. Di Colo, Mucoadhesive nanoparticles made of thiolated quaternary chitosan crosslinked with hyaluronan, Carbohydrate Polymers. 92 (2013) 33–39. doi:10.1016/j.carbpol.2012.09.029.
[20] K.F. Morris, C.S. Johnson, Diffusion-ordered two-dimensional nuclear magnetic resonance spectroscopy, J. Am. Chem. Soc. 114 (1992) 3139–3141. doi:10.1021/ja00034a071.
[21] K.F. Morris, C.S. Johnson, Resolution of discrete and continuous molecular size distributions by means of diffusion-ordered 2D NMR spectroscopy, J. Am. Chem. Soc. 115 (1993) 4291–4299. doi:10.1021/ja00063a053.
[22] R. Freeman, S. Wittekoek, Selective determination of relaxation times in high resolution NMR, Journal of Magnetic Resonance (1969). 1 (1969) 238–276. doi:10.1016/0022-2364(69)90065-1.
[23] X.Z. Shu, Y. Liu, Y. Luo, M.C. Roberts, G.D. Prestwich, Disulfide Cross-Linked Hyaluronan Hydrogels, Biomacromolecules. 3 (2002) 1304–1311. doi:10.1021/bm025603c.
[24] M.N. Khalid, L. Ho, F. Agnely, J.L. Grossiord, G. Couarraze, Swelling properties and mechanical characterization of a semi-interpenetrating chitosan, STP Pharma Sciences. 9 (1999) 359–364.
[25] Y. Zambito, G. Uccello-Barretta, C. Zaino, F. Balzano, G. Di Colo, Novel transmucosal absorption enhancers obtained by aminoalkylation of chitosan, European Journal of Pharmaceutical Sciences. 29 (2006) 460–469. doi:10.1016/j.ejps.2006.09.001.
[26] S. Dünnhaupt, J. Barthelmes, D. Rahmat, K. Leithner, C.C. Thurner, H. Friedl, A. Bernkop-Schnürch, S-Protected Thiolated Chitosan for Oral Delivery of Hydrophilic Macromolecules: Evaluation of Permeation Enhancing and Efflux Pump Inhibitory Properties, Mol. Pharmaceutics. 9 (2012) 1331–1341. doi:10.1021/mp200598j.
[27] E.J. Cabrita, S. Berger, DOSY studies of hydrogen bond association: tetramethylsilane as a reference compound for diffusion studies, Magn. Reson. Chem. 39 (2001) S142–S148. doi:10.1002/mrc.917.
[28] R. Mannhold, ed., Molecular drug properties: measurement and prediction, Wiley-VCH, Weinheim, 2008.